Acousto-electric current in graphene under the influence of electromagnetic waves

Nguyen Quyet Thang[1], Pham Duc Chinh[1], Nguyen Thi Thanh Nhan[1], Nguyen Vu Nhan[2], Nguyen Thu Huong[2*]

[1]Department of Theoretical Physics, Faculty of Physics, VNU University of Science, 334 Nguyen Trai, Thanh Xuan, Hanoi, Vietnam;
[2]Faculty of Basic Science, Air Defence-Air Force Academy, Doai Phuong, Hanoi, Vietnam.
[*]Corresponding author: huong146314@yahoo.com
Received 15 Mar. 2026; Revised 18 May 2026; Accepted 10 Aug. 2026; Published 25 Aug. 2026.
DOI: https://doi.org/10.54939/1859-1043.j.mst.113.2026.135-141

ABSTRACT

Two-dimensional graphene has garnered significant interest owing to its unique quantum behaviors stemming from a linear energy dispersion relation, with the acoustic-electric (AE) effect emerging as a key phenomenon driven by charge carrier dynamics under surface acoustic waves (SAW). Classical models based on the Boltzmann kinetic equation, effective at elevated temperatures, fall short in accounting for low-temperature experimental data. This work adopts the quantum kinetic equation approach to analyze the AE current in monolayer graphene subjected to combined SAW and electromagnetic waves (EMW). We derive an analytical formula for the AE current that fully captures the electron-acoustic phonon scattering via the deformation potential mechanism and elucidates SAW's role. Numerical simulations reveal the AE current's nonlinear rise with temperature, alongside sharp declines with increasing material sound velocity and EMW parameters. These trends highlight the potential for precise control of AE current via external stimuli. By advancing from classical to quantum frameworks, this study offers deeper insights into the AE effect's fundamentals in two-dimensional graphene.

Keywords: Acoustic-electric effect; Surface acoustic waves; Two-dimensional graphene; Electromagnetic waves; Quantum kinetic equation; Electron-acoustic phonon scattering.

1. INTRODUCTION

Graphene, a single-layer two-dimensional carbon structure, commands intense research focus due to its remarkable linear band structure, where charge carriers mimic massless Dirac fermions [1, 2]. This dispersion yields wavefunctions and spectra distinct from traditional semiconductors, enabling superior carrier mobility and quantum transport at ambient conditions. Such properties set graphene's quantum effects apart from conventional 2D electron gases, making electron-phonon scattering mechanisms, particularly via deformation potential, a cornerstone for both fundamental understanding and graphene-enabled nanoelectronics and optoelectronics.

A focal point is the acoustic-electric (AE) effect, where surface acoustic waves profoundly modulate graphene's transport via efficient momentum exchange with carriers, amplified by the material's high mobility and dispersion traits. Originally observed in 1950s bulk semiconductors, the primary mechanism for generating the current J_{AE} is the momentum transfer from the surface acoustic wave (SAW) phonons to the electron system through electron–phonon interaction, specifically via the deformation potential. Under the influence of SAW, electrons are pushed to one side in the direction of wave propagation, breaking the symmetry of the Fermi-Dirac distribution function, thereby creating a potential difference and generating a current. The AE effect through the deformation potential in propagating acoustic waves has been theoretically and experimentally explored in low-dimensional platforms such as quantum wells and superlattices [5, 6].

Early AE investigations emphasized external bulk acoustic waves (EAW) in thick semiconductors (e.g., Si, Ge, GaAs) and quantum structures [5], where EAW engages the full

material volume for stronger effects compared to SAW's surface-limited deformation potential interaction. Yet graphene's atomic-scale thinness favors SAW, enabling direct coupling to the lattice [9-11]. This shift supports graphene-based AE devices for GHz signal processing, sensors, and switches, leveraging SAW for carrier manipulation [14]. In this study, the EMW is not merely an external field but acts as a stimulating agent. The EMW alters the energy states of electrons and increases their transition probability when interacting with phonons. These demand quantum treatments beyond classical limits, especially under concurrent SAW and intense EMW driving [16].

Classical Boltzmann-based AE studies succeed at high temperatures but falter at low ones, overlooking quantum features like multi-photon scattering and coherence [6, 9]. Quantum kinetic equations, by contrast, model these along with field-phase dependencies crucially in graphene's low-temperature Dirac regime under dual SAW-EMW excitation. This expands theoretical reach across temperatures and quantifies EMW impacts on scattering. Building on prior classical and perturbative graphene AE work without external acoustics [9], we introduce a quantum kinetic framework incorporating SAW and EMW influences, valid broadly. EMW introduces nonlinearities reshaping deformation potential scattering probabilities, which our calculations numerically illustrate through AE current dependencies on EMW traits.

2. PROBLEM

The acoustic-electric current in two-dimensional graphene

In our model, a monolayer graphene sheet lies flat in the x-y plane, aligning precisely with the domain of unrestricted electron propagation. Carrier dynamics follow the 2D Weyl equation for massless Dirac fermions [1]. Consequently, the electron wavefunction and corresponding eigenenergies take the forms given in Ref [16]:

$$\Psi(\boldsymbol{p}) = \frac{\exp(i\boldsymbol{pr})}{L\sqrt{2}}\begin{pmatrix} n \\ e^{i\theta(\boldsymbol{p})} \end{pmatrix} \tag{1}$$

$$\Psi(\boldsymbol{p}) = \frac{\exp(i\boldsymbol{pr})}{L\sqrt{2}}\begin{pmatrix} n \\ e^{i\theta(\boldsymbol{p})} \end{pmatrix} \tag{2}$$

$$\varepsilon_{n,\boldsymbol{p}} = n\hbar v_f|\boldsymbol{p}|$$

Here, $n = \pm 1$ labels the conduction ($n = +1$) and valence ($n = -1$) bands; $\hbar$ is the reduced Planck's constant; v_f represents the Fermi velocity; $p = (p_x, p_y)$ denotes the in-plane momentum of carriers in the graphene sheet; $r = (x, y)$ is the position vector in 2D space; θ gives the angle between p and the propagation direction; and $L_x = L_y = L$ sets the normalization length along each system axis.

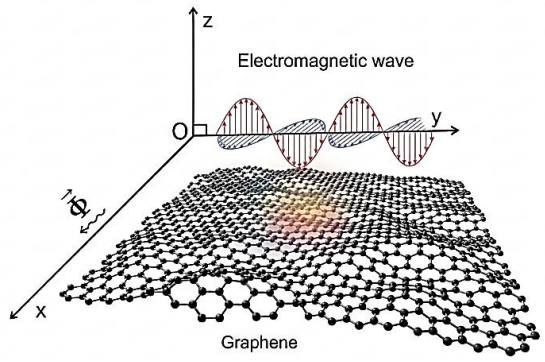

Figure 1. *Schematic representation of the acousto-electric effect in the presence of an electromagnetic wave.*

When an electromagnetic wave propagates along the y-axis, its electric field takes the form $E =$

$(0, E_0 \sin(\Omega t), 0)$, where E_0 and Ω represent the intensity and frequency of electromagnetic waves, respectively. Under these conditions, the Hamiltonian describing the electron-acoustic phonon interaction in monolayer graphene is expressed in second-quantized form as detailed in Ref [4]:

$$H = \sum_{n,\boldsymbol{p}_\perp} \varepsilon_n \left(\boldsymbol{p}_\perp - \frac{e}{\hbar c} \boldsymbol{A}(t) \right) a^\dagger_{n,\boldsymbol{p}_\perp} a_{n,\boldsymbol{p}_\perp} + \sum_{\boldsymbol{k}} \hbar \omega_{\boldsymbol{k}} \left(b^\dagger_{\boldsymbol{k}} b_{\boldsymbol{k}} + \frac{1}{2} \right) + \sum_{n,n'} \sum_{\boldsymbol{p}_\perp,\boldsymbol{k}} C(k) a^\dagger_{n',\boldsymbol{p}_\perp+\boldsymbol{k}_\perp} a_{n,\boldsymbol{p}_\perp} \left(b^\dagger_{-\boldsymbol{k}} + b_{\boldsymbol{k}} \right) + \sum_{n,n'} \sum_{\boldsymbol{p}_\perp,\boldsymbol{q}} C(q) U_{n,n'}(\boldsymbol{q}) a^\dagger_{n',\boldsymbol{p}_\perp+\boldsymbol{q}_\perp} a_{n,\boldsymbol{p}_\perp} b_{\boldsymbol{q}} e^{-i\omega_{\boldsymbol{q}} t} \quad (3)$$

where $a^\dagger_{n',\boldsymbol{p}\perp+\boldsymbol{k}\perp}$ and $a_{n,\boldsymbol{p}\perp}$ ($b^\dagger_{\boldsymbol{k}}$ and $b_{\boldsymbol{k}}$) represent the creation/annihilation operators for electrons (phonons). The kets $|n, \boldsymbol{p}_\perp\rangle$and $|n', \boldsymbol{p}_\perp + \boldsymbol{k}_\perp\rangle$ denote the electron's initial and final scattering states, respectively. The laser's vector potential, modeled as EMW, reads $A(t) = \frac{c}{\Omega} E_0 \cos(\Omega t)$, with c as the speed of light in vacuum. Here, ω_k and ω_q signify the frequencies of intrinsic and external acoustic phonons, respectively. $U_{n,n'}(q)$ is the matrix element of the operator $U = \exp(i\boldsymbol{qr})$ as follows $\left|U_{n,n'}(q)\right|^2 = \frac{1}{2}[1 + \cos(\theta)]$ [13]. Within the deformation potential framework, $C(k)$ represents the coupling strength for electron-intrinsic acoustic phonon interactions [10]:

$$|C(k)|^2 = \frac{\hbar^2 v_s k}{\tau_{DA}} \quad (4)$$

where $\tau_{DA} = \frac{2\hbar\rho v_s^2}{\Xi^2}$, with Ξ as the deformation potential coupling constant. Similarly, $C(q)$ characterizes the electron-external acoustic phonon (SAW) interaction strength [13]:

$$|C(q)|^2 = \frac{\hbar D_{ac}^2 q}{2\rho v_s L^2} \quad (5)$$

where D_{ac} represents the deformation potential coupling constant, while ρ and v_s denote the 2D graphene mass density and longitudinal sound velocity within the graphene sheet, respectively.

The general quantum kinetic equation for the electron distribution function in two-dimensional graphene is given by:

$$i\hbar \left(\frac{f_{n,\boldsymbol{p}_\perp(t)}}{\partial t} \right) = i\hbar \langle \left[a^\dagger_{n,\boldsymbol{p}_\perp} a_{n,\boldsymbol{p}_\perp}, H \right] \rangle_t \quad (6)$$

Starting from the Hamiltonian in Equations (3) and (6), we perform the necessary operator manipulations to derive the solution. This yields the quantum kinetic equation governing electrons in two-dimensional graphene $f_{n,\boldsymbol{p}\perp}$. To compute the acoustic-electric current, we first determine the current density j_{AE}. The quantum AE current j_{AE}, aligned with the external acoustic wavevector q, takes the form given in Ref [5]:

$$j_{AE} = e \sum_{n,p_\perp} v_p \, f_{n,\boldsymbol{p}\perp} \quad (7)$$

where e represents the electron charge. The carrier velocity v_p follows from the relation $v_p = \frac{1}{\hbar} \frac{\partial \varepsilon_{n,p}}{\partial p}$ as detailed in Ref [5]. Assuming τ_0 remains constant throughout, we derive the explicit expression for the AE current as: Substituting the interaction coefficients and converting the momentum sum to an integral over phase space simplifies the scattering rate expression. Further

application of Dirac delta function properties [17] enables energy integration, yielding the analytical AE current formula:

$$j_{AE} = \frac{ev_f\tau_0\beta\hbar v_s S}{16\pi\tau_{DA}} N_k \left(-\frac{3}{2\kappa^4}\right)[(1-2\alpha^2)(Q_+^0+Q_-^0)+\alpha^2(Q_+^1+Q_-^1+Q_+^{-1}+Q_-^{-1})] + \frac{ev_f\tau_0\beta D_{ac}^2 S}{32\pi\rho v_s} N_q \left(-\frac{3}{2\kappa^4}\right)[(1-2\alpha^2)P^0+\alpha^2(P^1+P^{-1})] \quad (8)$$

where

$$\kappa = \frac{\beta\hbar v_f}{4} \quad (9)$$

$$Q_\pm^x = \mathrm{Li}_3\left(-\exp\left[-\beta\left(\frac{x\hbar\Omega}{2}\pm\frac{\hbar\omega_k}{2}-\varepsilon_f\right)\right]\right) \quad (10)$$

$$P^x = \mathrm{Li}_3\left(-\exp\left[-\beta\left(\frac{x\hbar\Omega}{2}+\frac{\hbar\omega_k}{2}-\frac{\hbar\omega_q}{2}-\varepsilon_f\right)\right]\right) \quad (11)$$

where ε_F characterizes the Fermi energy scale, and $\mathrm{Li}_n(x)$ represents the polylogarithm function of order n. The system area is defined as $S = L^2$. $N_k = \frac{1}{\exp\left(\frac{\hbar\omega_k}{k_BT}\right)-1}$, with k_B as Boltzmann's constant and T the system temperature. For external phonons, $N_q = \frac{SI_{\mathrm{SAW}}}{\hbar\omega_q v_s}$, where $I_{\mathrm{SAW}} = \frac{1}{2}\rho_S V_0^2 \omega_q^2 v_s$. τ_0 denoting the momentum relaxation time.

Numerical evaluation of Eq.(8), obtained via quantum kinetic equations, reveals intricate electron-acoustic phonon scattering dynamics under combined SAW-EMW driving through deformation potential interactions showing richer dependencies than classical Boltzmann approaches. The subsequent section presents comprehensive numerical computations across wide parameter ranges, visualized graphically to elucidate AE current variations with temperature, SAW frequency, EMW characteristics, and substrate choices.

3. RESULTS AND DISCUSSION

3.1. Input data

In order to elucidate the findings obtained, the present section focuses on the acousto-electric current. The analysis is carried out with respect to its dependence on the temperature T, the electromagnetic wave frequency Ω, as well as the intrinsic parameters of two-dimensional graphene. For the numerical evaluations, the adopted parameters are [9, 10]: $e = 1.60219 \times 10^{-19} C$, $D_{ac} = 9$ eV, $v_s = 2.1 \times 10^4$ m/s, $\rho = 7 \times 10^{-7}$ kg/m^2, $L = 20$ nm, $v_f = 2 \times 10^6$ m/s, $\Xi = 6.8$ eV, $\tau_0 = 10^{-10} s$

3.2. Simulation results and comments

Figure 2(a) illustrates the variation of the acousto-electric current j_{AE} with temperature T for different electromagnetic wave intensities via the deformation potential mechanism [18]. The quantum kinetic model reveals a strong nonlinear rise in I_{AE} with T, featuring the most rapid growth below 30 K. The study [9] also shows the results of AE current increasing rapidly at low temperatures.

Temperature modulates the AE current through dual channels. Phonon population grows via Bose-Einstein statistics as $N_{\boldsymbol{k}} = [\exp(\hbar\omega_k/k_BT)-1]^{-1}$, boosting electron-phonon scattering rates and thus momentum transfer efficiency evident in the current prefactors $j_{AE} \propto N_{\boldsymbol{k}}, N_{\boldsymbol{q}}$ (Eq.8), consistent with prior studies [7]. Additionally, elevated T broadens the electron distribution near ε_F, recruiting more carriers into scattering processes [12].

Figure 2(b) displays how the acousto-electric current with EMW frequency Ω across multiple temperature conditions through deformation potential coupling. All curves show characteristic decay with rising Ω, featuring sharp drops at low frequencies and saturation plateaus at high frequencies.

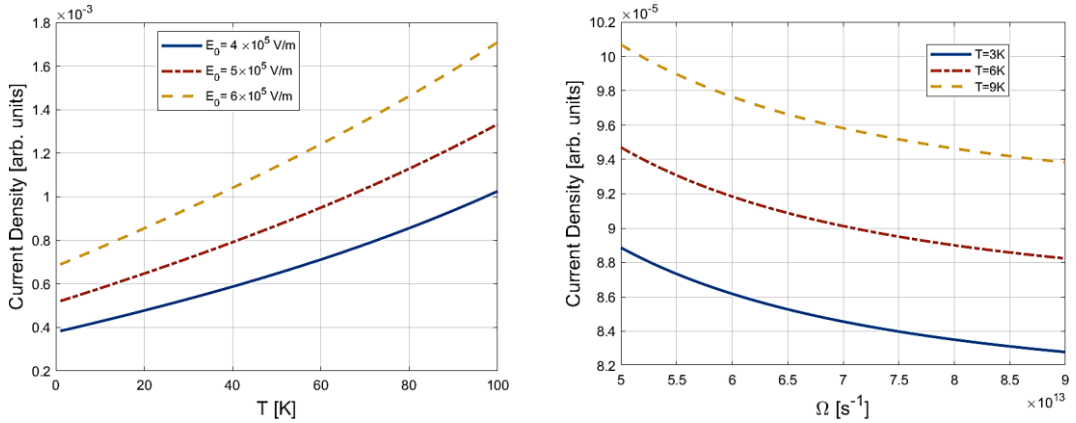

Figure 2. *Dependence of the acousto-electric current on (a) temperature T for different electromagnetic wave intensities and (b) electromagnetic wave frequency Ω at different temperatures.*

This dependence originates from the way the electromagnetic wave frequency Ω governs the arguments of the Bessel functions within the quantum kinetic equations. With the field amplitude held constant, an increase in Ω results in smaller arguments for these functions. This suppresses the contribution of higher-order terms, leading to a monotonic reduction in the current magnitude. Physically, the rapid oscillations of the electromagnetic field at high frequencies limit the efficiency of electron momentum gain. Because the field reverses direction so quickly, the electrons cannot be effectively accelerated in a single direction, thereby reducing the overall net current [8].

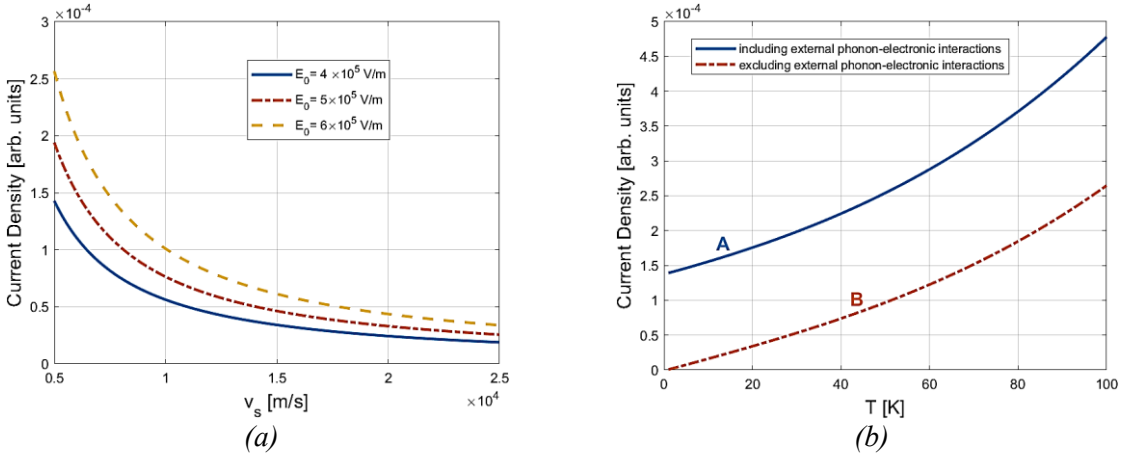

Figure 3. *The Dependence of the acousto-electric current on (a) sound wave velocity v_s for different electromagnetic wave intensities and (b) temperature T in the presence and absence of electromagnetic waves.*

Figure 3(a) illustrates the dependence of the AE current on the sound velocity v_s reflecting the mechanical nature of the material. Physically, $v_s$is proportional to the stiffness of the material; higher values of v_s characterize materials with high elasticity and a stable lattice structure [19]. A lattice with high stiffness will be less sensitive to mechanical deformations caused by acoustic waves, leading to a reduction in the electron-phonon coupling strength. As a result, even though the input acoustic energy increases, the efficiency of momentum transfer from phonons to the electronic system remains limited, causing a decrease in the AE current.

Figure 3(b) illustrates the temperature dependence of the acousto-electric current for the case

without the EMW (E_0=0 W/m); specifically, curve (A) represents the case considering external electron–phonon interaction, while curve (B) represents the case neglecting it. In the absence of the EMW (E_0=0 W/m) and without external electron–phonon interaction, the investigation conditions are identical to those in Ref [9]. When observing the temperature dependence of the acousto-electric current, we find a qualitative similarity between the graph currently under investigation and the results in Ref [9].

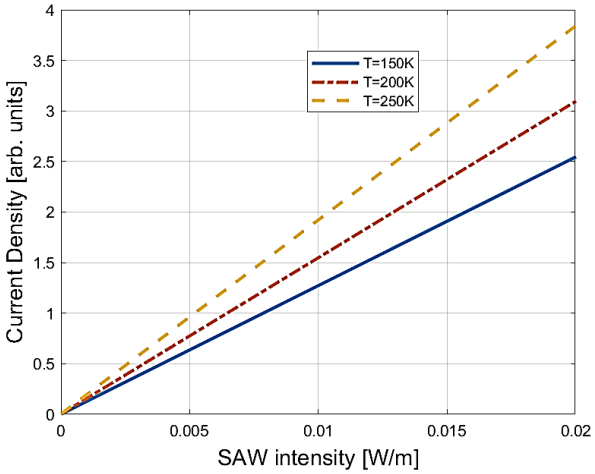

Figure 4. *The effect of SAW intensity on the acousto-electric.*

Figure 4 illustrates the influence of the SAW intensity on the acousto-electric effect; it is observed that as the acoustic wave intensity increases, the current density also increases. When compared with graph 2 in ref [19], a similar trend was observed.

4. CONCLUSIONS

We present a quantum kinetic theory for the acousto-electric current in monolayer graphene under combined surface acoustic wave and electromagnetic wave excitation. The derived analytical expression fully describes electron-acoustic phonon scattering through the deformation potential mechanism, revealing nonlinear transport characteristics and low-temperature quantum coherence effects beyond classical Boltzmann transport limitations.

Comprehensive parameter sweeps demonstrate highly flexible control of AE current magnitude across multiple orders through temperature, phonon frequencies, sound velocity, and EMW characteristics. These findings establish quantitative design guidelines for graphene-based acousto-electronic devices, highlighting optimal material selection and multi-parameter tuning strategies. The formalism extends naturally to other 2D Dirac materials, providing a robust theoretical foundation for quantum acousto-electric transduction in low-dimensional systems.

Acknowledgement: *This research is financially supported by Vietnam National University, Hanoi - Grant Number QG.26.41 (by PhD. Nguyen Thi Thanh Nhan): "Quantum Theory of Influence of Strong Electromagnetic Wave on some optical, electric and magnetic Properties of Two-dimensional Dirac Semiconductor Materials (Graphene, Borophene)".*

REFERENCES

[1]. T. Ando, "*Theory of electronic states and transport in carbon nanotubes*", Journal of the Physical Society of Japan, Vol. 74, No. 3, pp. 777–817, (2005).

[2]. S. A. Yang, "*Dirac and Weyl materials: Fundamental aspects and some spintronics applications*", Spin, Vol. 6, No. 2, (2016).

[3]. Vl. A. Margulis and E. E. Muryumin, "*Giant quantum oscillations of acoustoelectric current in narrow graphene nanoribbons*", Journal of Physics D: Applied Physics, Vol. 57, No. 7, p. 075304, (2024).

[4]. Vl. A. Margulis and E. E. Muryumin, "*Surface acoustic wave amplification by drifting electrons in semiconducting epitaxial graphene on silicon carbide*", Journal of Physics D: Applied Physics, Vol. 58, No. 1, p. 015308, (2025).
[5]. N. V. Hieu et al., "*The influence of the electromagnetic wave on the nonlinear quantum acoustoelectric current in a quantum well*", Progress In Electromagnetics Research, p. 541, (2013).
[6]. S. Y. Mensah, F. K. A. Allotey and N. G. Mensah, "*Nonlinear acoustoelectric effect in a semiconductor superlattice*", Journal of Physics: Condensed Matter, Vol. 12, No. 24, pp. 5225–5232, (2000).
[7]. B. K. Ridley, "*Quantum processes in semiconductors*", Oxford University Press, (2013).
[8]. N. W. Ashcroft and N. D. Mermin, "*Solid state physics*", p. 403, (1976).
[9]. S. Nafees et al., "*Acoustoelectric current in graphene due to electron deformation potential and piezoelectric phonon couplings*", Physica Scripta, Vol. 97, No. 4, p. 045705, (2022).
[10]. S. H. Zhang et al., "*Piezoelectric surface acoustical phonon limited mobility of electrons in graphene on a GaAs substrate*", Physical Review B—Condensed Matter and Materials Physics, Vol. 87, No. 7, p. 075443, (2013).
[11]. V. Miseikis et al., "*Acoustically induced current flow in graphene*", Applied Physics Letters, Vol. 100, No. 13, (2012).
[12]. S. Mayorov et al., "*How close can one approach the Dirac point in graphene experimentally?*", Nano Letters, Vol. 12, No. 9, pp. 4629–4634, (2012).
[13]. S. Adam et al., "*Theory of charged impurity scattering in two-dimensional graphene*", Solid State Communications, Vol. 149, No. 27–28, pp. 1072–1079, (2009).
[14]. S. Okuda et al., "*Graphene surface acoustic wave sensor for simultaneous detection of charge and mass*", ACS Sensors, Vol. 3, No. 1, pp. 200–204, (2018).
[15]. Y. Mou et al., "*Coherent detection of the oscillating acoustoelectric effect in graphene*", Physical Review Letters, Vol. 134, No. 9, p. 096301, (2025).
[16]. T. A. Tuan et al., "*Two-dimensional graphene: Theoretical study of multi-photon non-linear absorption coefficient of a strong electromagnetic wave by using quantum kinetic equation*", Journal of the Physical Society of Japan, Vol. 92, No. 6, p. 064401, (2023).
[17]. W. M. Hartmann, "*Signals, sound, and sensation*", Springer Science & Business Media, pp. 154–155, (2004).
[18]. L. Bandhu and G. R. Nash, "*Temperature dependence of the acoustoelectric current in graphene*", Applied Physics Letters, Vol. 105, No. 26, (2014).
[19]. R. Hanus et al., "*Lattice softening significantly reduces thermal conductivity and leads to high thermoelectric efficiency*", Advanced Materials, Vol. 31, No. 21, p. 1900108, (2019).

TÓM TẮT

Dòng âm điện trong graphene dưới tác động của sóng điện từ

Graphene hai chiều đã thu hút sự quan tâm đáng kể nhờ các hành vi lượng tử độc đáo bắt nguồn từ quan hệ tán sắc năng lượng tuyến tính, trong đó hiệu ứng âm - điện (AE) nổi lên như một hiện tượng then chốt được thúc đẩy bởi động lực học của hạt tải điện dưới tác động của sóng âm bề mặt (SAW). Các mô hình cổ điển dựa trên phương trình động học Boltzmann, vốn hiệu quả ở nhiệt độ cao, đã không thể giải thích thỏa đáng các dữ liệu thực nghiệm ở nhiệt độ thấp. Nghiên cứu này áp dụng phương pháp phương trình động học lượng tử để phân tích dòng AE trong Graphene đơn lớp chịu tác động kết hợp của SAW và sóng điện từ (EMW). Chúng tôi thiết lập một công thức giải tích cho dòng AE, phản ánh đầy đủ sự tán xạ electron-phonon âm thông qua cơ chế thế biến dạng và làm sáng tỏ vai trò của SAW. Các mô phỏng số cho thấy dòng AE tăng phi tuyến theo nhiệt độ, đồng thời giảm mạnh khi vận tốc âm trong vật liệu và các tham số EMW tăng lên. Những xu hướng này nhấn mạnh tiềm năng điều khiển chính xác dòng AE thông qua các kích thích bên ngoài. Bằng cách tiến triển từ khung lý thuyết cổ điển sang lượng tử, nghiên cứu này mang lại cái nhìn sâu sắc hơn về các nguyên lý cơ bản của hiệu ứng AE trong Graphene hai chiều.

Từ khoá: Hiệu ứng âm – điện; Sóng âm bề mặt; Graphene hai chiều; Sóng điện từ; Phương trình động học lượng tử; Tán xạ điện tử-phonon âm.